

# Numerical and parametric study of a centrifugal pump

## Effect of blade number and volute shape

[ Javad abolfazli esfahani, Behrooz Jamshidi Moghadam, Mohammadmojtaba Nouri and Amirreza Mahmoudi ]

**Abstract**—Various parameters affect the pump performance in which blade number, blade angle, outlet diameter, and volute shape are the most important. In this paper the performance of pumps with different impellers containing blade number and different volute shape containing circular-elliptical and rectangular is evaluated. In this study four different blade numbers 5, 6, 7, and 8 are modeled and two different rectangular and circular-elliptic volute shapes are also studied. Incompressible Navier-Stokes equations over a hybrid grid is solved by commercial software package Fluent. Rotational zone will be simulated by moving reference frame method. For each impeller, the flow pattern and pressure distribution are calculated and finally the head and efficiency curves are compared and discussed. The results show that by increasing the blade number the head increase and efficiency decrease slightly. Also circular-elliptic volute shows better performance especially in higher flow rates than the rectangular one.

**Keywords**—centrifugal pump, blade number, volute shape, moving reference frame, Fluent

### I. Introduction

Centrifugal pump is one of the most most important pump kinds in industry and agriculture applications [1]. The principal of this pump kind is based on centrifugal force. Rotation of impeller exerts centrifugal force to pump liquid and it causes liquid to go out of impeller with higher velocity. This relative vacuum takes the pump liquid into the impeller. Pump liquid has high velocity at the impeller exit, so for converting this velocity to pressure volute is used. Refer to [2] for more information about this kind of pumps and its classification.

Usually, CFD codes simulate turbo machinery flows in three ways containing the multiple reference frame (MRF) used in this paper, the mixing plane and the sliding mesh. The first two methods are used for steady problem and solver, but the third one is used for unsteady simulation. In MRF method nothing rotates other than reference frame. This means that rotation is modeled by rotating reference frame but fixed grid. This fixed grid is accompanied with sooner convergency and less computational cost. Rotating reference frame causes centrifugal and coriolis accelerations.

CFD analyses have been done in this field by various commercial codes containing CFX-TASCflow by Kaupert et al. [4], Fluent by Potts and Newton [5] and STARCD by Sun and Tsukamoto [6].

Experiments have shown that the number of impeller blades has a significant influence on the performance of a centrifugal pump [7] but as the viscosity of pumped liquid increases this effect weakens [8].

According to experiments the shape of pump volute has noticeable impact on the performance of a centrifugal pump [9].

This study is related to influence of blade number and volute shape on the centrifugal pump performance. The computational fluid dynamic is done by Fluent software package [10], used enormously in turbo machinery fields and have been proven by Sun et al. [11] and Gonzalez et al. [12] to be reliable.

## II. Main Text

### A. Geometry of the pump used

Preparing the geometry of four impellers with different blade number and two different volute shapes was done in Ansys BladeGen software. In this paper four different impellers with the same shape but different blade numbers 5, 6, 7 and 8 and two different volute shape with 6 bladed impeller have been studied. Other configurations of the pump are listed below in "Table 1". It should be noted that all angles are measured from tangent.

### B. Governing equations and turbulence

The incompressible flow through the rotating impeller is solved in a moving frame of reference with constant rotational speed equal to the rotational speed of the impeller. The flow through the stationary parts of the pump is solved in an inertial reference frame. The governing equations for the impeller are formulated below:

$$\nabla \rho u_r = 0 \quad (1)$$

$$\nabla \rho u_r + 2\rho\Omega \times u_r + \rho\Omega \times \Omega \times r = -\nabla p + \mu_{eff} \nabla^2 u_r \quad (2)$$

Javad Abolfazli Esfahani, professor of mechanical engineering  
Ferdowsi university of Mashhad  
Iran

Behrooz Jamshidi Moghadam, M. Sc. student of mechanical engineering  
Ferdowsi university of Mashhad  
Iran

Mohammadmojtaba Nouri and Amirreza Mahmoudi, bachelor of science students of mechanical engineering  
Ferdowsi university of Mashhad  
Iran

Table 1. General configurations of the pump used in this study

Impeller	Hub leading edge blade angle(deg)		27
	Mean leading edge blade angle(deg)		19
	Shroud leading edge blade angle(deg)		16
	Exit blade angle (deg)		22.5
	Inlet eye diameter (mm)		45.05
	Shaft diameter (mm)		15.63
	Outlet diameter (mm)		119.62
Volute	Circular& elliptic	Outlet area (mm <sup>2</sup> )	2336
		Tongue clearance (mm)	12.365
		Base circle radius (mm)	125.81
	rectangular	Outlet area (mm <sup>2</sup> )	2286
		Tongue clearance (mm)	12.365
		Base circle radius (mm)	125.81

$$\mu_t = \rho C_m \frac{k^2}{\varepsilon} \quad (6)$$

where  $u$  is the local velocity vector,  $k$  is the turbulent kinetic energy,  $\varepsilon$  is the dissipation rate,  $\mu$  is the laminar viscosity,  $\mu_t$  is the turbulent viscosity,  $G_k$  represents the generation of turbulent kinetic energy due to the mean velocity gradients,  $\sigma_k = 1$  and  $\sigma_\varepsilon = 1.2$  are the turbulent Prandtl numbers and  $C_{1\varepsilon} = 1.44$ ,  $C_{2\varepsilon} = 1.92$  and  $C_m = 1.92$  are the constants of the model.

Head of the pump is derived from the formulation below:

$$h = \frac{P_{tot,out} - P_{tot,in}}{\rho g} \quad (7)$$

$$P_{tot} = P_{static} + P_{dynamic} \quad (8)$$

where  $h$  is head,  $p_{tot,out}$  is the average total pressure at the volute exit,  $p_{tot,in}$  is the average total pressure at the eye of the impeller,  $\rho$  is the water density equal to  $1000 \frac{kg}{m^3}$  and  $g$  is the earth global attraction acceleration equal to  $9.8 \frac{m}{s^2}$ .

Also hydraulic efficiency meaning energy output divided by energy input is calculated from below equation:

$$\eta = \frac{Output \ power}{Input \ power + Mechanical \ losses \ power} \quad (9)$$

Although hydraulic losses are calculable in numerical simulations, mechanical losses could not be assessed by numerical simulation of fluid flow. So our numerical hydraulic efficiency is higher in value than real due to absence of mechanical losses. Thus the hydraulic efficiency in this study is calculated by following equation:

$$\eta = \frac{\dot{m}gh}{T\Omega} \quad (10)$$

which  $T$  is the torque needed to rotate the impeller at constant desired rotational speed and is calculated by numerical calculation,  $\dot{m}$  is the mass flow rate of pumping system in  $kg/s$ . As mentioned before  $\Omega$  is the rotational velocity in  $rad/s$ .

### C. Mesh generation and boundary conditions

In this study hybrid mesh has been used. The impeller and volute have hexagonal and tetrahedron grid, respectively. The impeller mesh is produced by Ansys Turbo-grid and volute mesh by Ansys Geometry. A grid view of the impeller mesh is presented in Fig. 1.

where  $\rho$  is the density of the fluid,  $p$  is the static pressure,  $u_r$  is the vector fluid velocity in the rotating system,  $\Omega$  is the rotational speed and  $\mu_{eff}$  is the dynamic effective viscosity derived from model of turbulence. The last two terms in the left hand side of equation (2) are the effects of the Coriolis and centrifugal forces due to the rotating frame of reference.

For the stationary parts of the centrifugal pump, the governing equations are formulated in the stationary reference frame. The continuity equation remains the same, but the momentum equation reduces to:

$$\nabla \rho u = -\nabla p + \mu_{eff} \nabla^2 u \quad (3)$$

where  $u$  is the vector fluid velocity in the stationary frame of reference.

The turbulence of the flow is modeled with standard  $k - \varepsilon$  model with realizable sub model that is rated as the most used model that combines simplicity, robustness and reasonable accuracy. Moreover, it has been tested in a wide range of industrial flows showing satisfactory results. The differential transport equations for the turbulence dissipation rate are:

$$\nabla \rho u k = \nabla \left( \left( \mu + \frac{\mu_t}{\sigma_k} \right) \nabla k \right) + G_k - \rho \varepsilon \quad (4)$$

$$\nabla \rho u \varepsilon = \nabla \left( \left( \mu + \frac{\mu_t}{\sigma_\varepsilon} \right) \nabla \varepsilon \right) + C_{1\varepsilon} \frac{\varepsilon}{k} G_k - C_{2\varepsilon} \rho \frac{\varepsilon^2}{k} \quad (5)$$

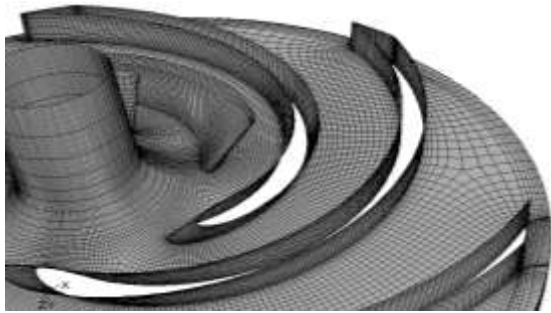


Figure 1. Top view of structured hexagonal mesh in impeller

Rotating wall with zero rpm angular velocity relative to adjacent cell zone for blade and hub walls, mass flow inlet for inlet of the pump, stationary wall for shroud and volute and pressure outlet for exit of volute have been set as boundary conditions. The impeller zone rotates with constant angular velocity of 2900 rpm.

#### D. Flow solution and solver settings

The CFD commercial code Fluent has been used to solve three dimensional viscous incompressible flow. "Table 2" shows the details of solver setup. In addition of residuals to be lower than  $10^{-4}$ , we continue the solution to achieve approximately fix head for the last 100 iterations.

According to our experience in  $k-\varepsilon$  turbulence model, realizable sub model shows more robust solution and better convergence than standard and RNG models.

#### E. Grid independency and validation

Grid independency and validation are the two important criteria of every CFD work. In this paper, grid independency has been done for every of four pumps. Because of complexity and volume of calculations, grid independency was taken only for  $80 \text{ m}^3/\text{hr}$  volume flow rate. The head is the criterion for judging the grid independency. Thus number of cells for 5, 6, 7 and 8 are 776655, 659550, 669924 and 727646, respectively. Complete information about grid independency are gathered in "Table 3".

The pump used in this study is a typical pump and it does not have experimental data to validate with. Thus we have validated our solution procedure for K 32-200 centrifugal

pump. Comparison of numerical and experimental head is presented in Fig. 2. We see that by increase of flow rate

Table 2. Details of solver settings

Solver	Steady, Pressure based
Turbulence model	Realizable $k-\varepsilon$
Near wall treatment	Standard wall functions
Pressure-Velocity coupling	SIMPLE
Pressure	Standard
Discretization scheme for convective fluxes and turbulence parameters	Second order upwind

Table 3. Detailed information of grid independency

Blade number	Impeller and inlet cell NO. (hexagonal)	Volute cell NO. (tetrahedron)	Total cell NO. (hybrid)	Head (m)
5	386630	130890	517520	64.91
	✓ 579945	196710	776655	62.10
	858320	293455	1151775	62.01
6	308557	130890	439447	66.34
	✓ 462840	196710	659550	63.67
	694260	293455	987715	63.45
7	314567	130890	445457	68.93
	✓ 473214	196710	669924	66.67
	709821	293455	1003276	66.34
8	354467	130890	485357	69.06
	✓ 530936	196710	727646	66.67
	795345	293455	1088800	66.40

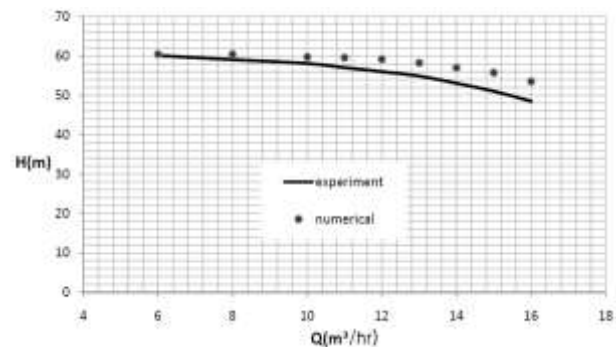


Figure 2. Comparison of numerical and experimental head-capacity

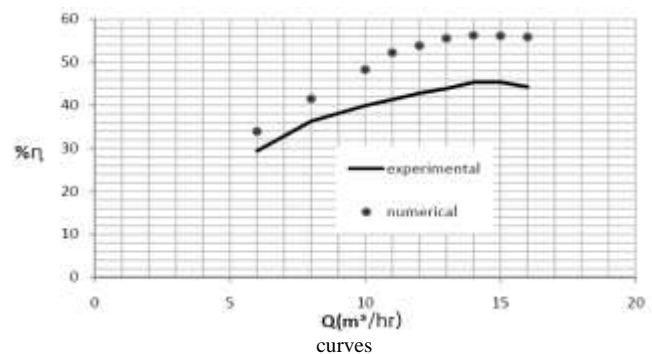


Figure 3. Comparison of numerical and experimental efficiency curves

the accuracy of numerical head will decrease. This may be due to increase of complexity of flow, reversed flows, and pressure pulsations which numerical method cannot capture them as well as low volume flow rates.

The comparison between numerical and experimental efficiency of the 32-200 centrifugal pump is presented in Fig. 3. As it could be seen, the difference between numerical and experimental efficiency is rather high. This is because of neglected mechanical losses, which has been described in previous section, and higher head prediction. Both of these factors cause to predict numerical efficiency higher than

experimental efficiency, but the first one has more effect than the second one.

### III. Results and discussion

#### A. Effect of varying blade number

Head-capacity curves are presented in Fig. 4. It can be concluded that for our typical centrifugal pump by increasing the blade numbers from 5 to 8, head of the pump increase significantly. This increase of head is more significant in lower volume flow rates. But for volume flow rates higher than 80m<sup>3</sup>/hr, 7-bladed centrifugal pump produce higher head rather than 8-bladed one. Maybe this is due to more than enough occupation of fluid passage by blades in 8-bladed centrifugal pump.

In Fig. 5 efficiency curves of different bladed centrifugal pumps is presented. As seen by increasing the blade number, efficiency decreases. According to equation (10) head and moment are the two distinguisher factors of numerical efficiency value. Although by increasing blade number the pump produces more head, the moment needed to rotate rotor, containing of blades and hub, at constant rotational speed of 2900rpm increases too. The pump with more blade number has lower efficiency, this shows that moment increase overweight head increase.

In Fig. 6 the moment exerted on impeller is presented. This figure shows that the pump with more blade number needs more moment to rotate at constant rotational velocity of 2900rpm. So if we divide these values by the blade number, we have the needed moment for every blade which is presented in Fig. 7. This figure shows that one blade of the pump with fewer blade number needs more moment than the one with higher blade number.

An important conclusion derived from Fig. 7 is that by increasing the blade number the moment exerted on every blade decreases, so according to machine design statements by increasing the blade number we can decrease the blade thickness. This action prevents of increasing impeller weight and the flow passage opens more.

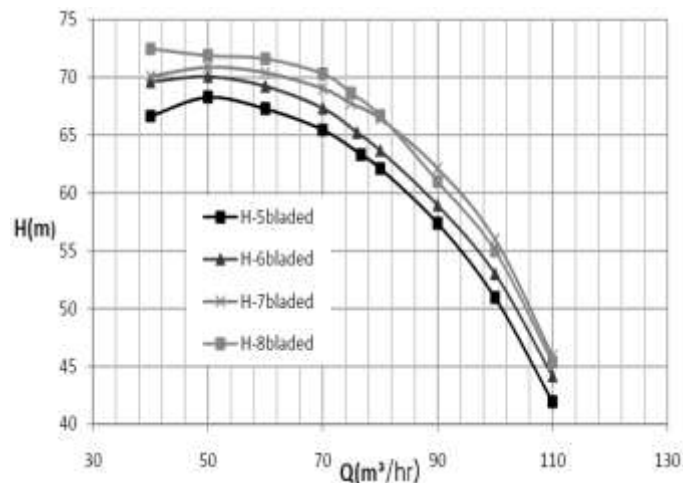


Figure 4. Head-capacity curves of different bladed impellers

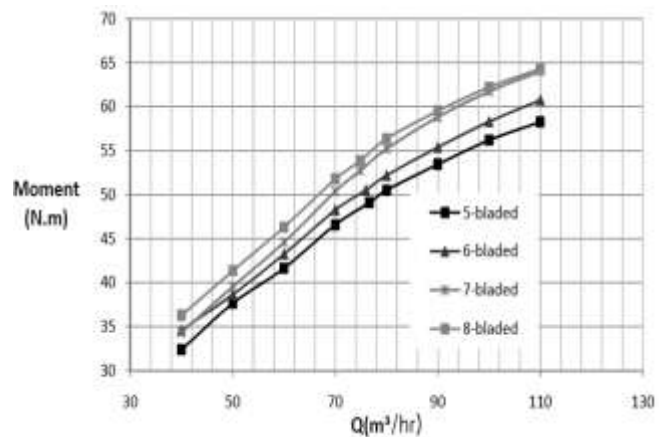
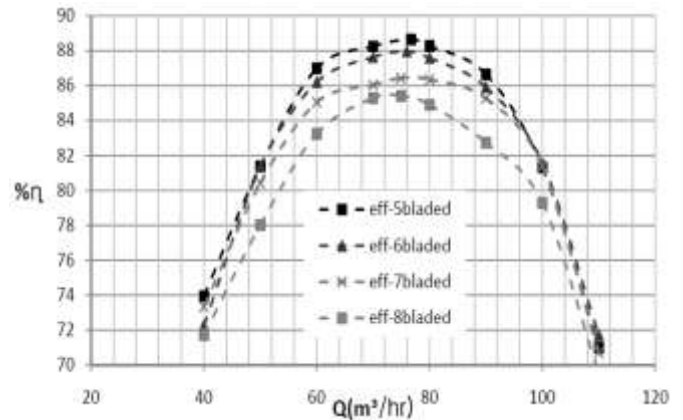


Figure 5. Efficiency curves of different bladed impellers

Figure 6. Moment needed of different bladed impellers at constant rotational velocity of 2900rpm

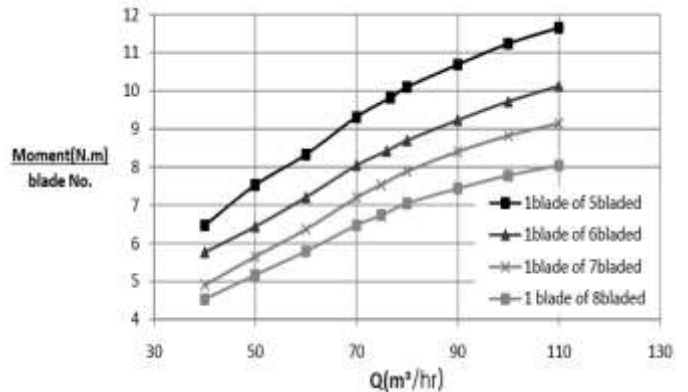


Figure 7. Moment needed of every blade of different bladed impellers at constant rotational velocity of 2900rpm

#### B. Effect of volute shape

Head-capacity curves are presented in Fig. 8. It is obvious that in all ranges of volume flow rates circular-elliptic volute produce more head than rectangular one. Also by increasing the volume flow rate, this discrepancy increase. But this



increase of head is not as much as to judge that circular-elliptic volute is better than rectangular one.

- By increasing the blade number head of the pump increases slightly, but it will be recompensed by decrease of efficiency.
- The moment needed to rotate impeller at constant rotational velocity of 2900 rpm increases by increase of blade number,

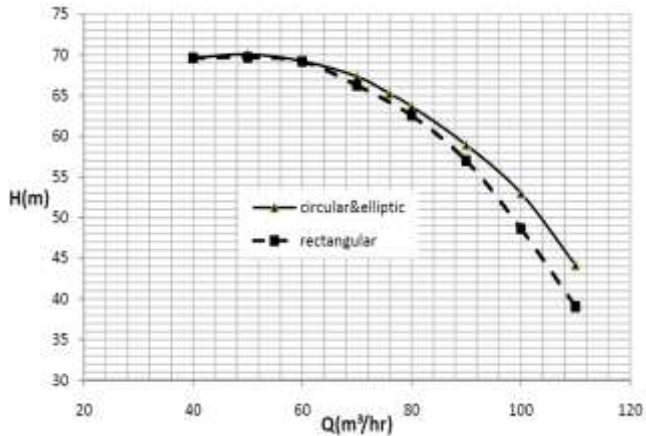


Figure 8. Head-capacity curves of pumps with different volutes

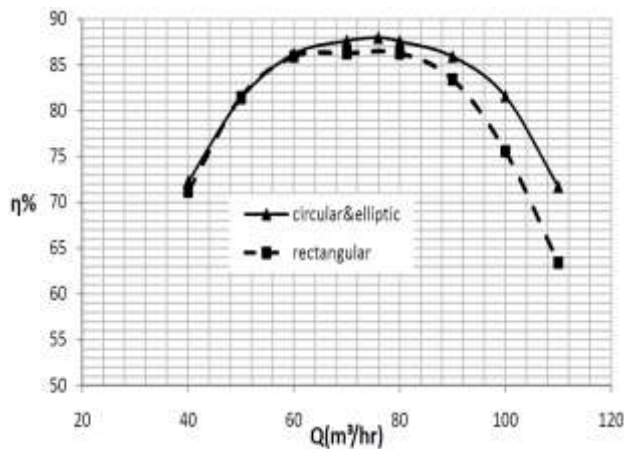


Figure 9. efficiency curves of pumps with different volutes

Fig. 9 shows efficiency charts of the two pumps. As like as head of the pump, by increasing the flow rate, the pump with circular-elliptic volute has better efficiency. May be one of this efficiency increase reasons is that the pump with rectangular volute has more surface than the circular-elliptic one causing more skin friction and consequently less efficiency.

#### iv. Conclusion

In this study four different bladed impellers with 5, 6, 7 and 8 blades and also two different rectangular and circular-elliptical volutes have been studied. The only different geometry parameter is the number of blades, so other parameters such as hub and shroud profiles, blade curvatures and so on are the same. The concluded remarks are listed as below:

this shows that impeller with more blade number exert more moment to fluid and consequently cause to produce more head. Reversely the moment for each blade decreases with increase of blade number. This shows that by increasing the blade number the moment exerted on every blade decreases so thinner blades can be used.

- By increasing the blade number fluid passes more smoothly through the passage, but from the other hand more surface friction and impeller volume occupation cause decrease in efficiency.

- By increasing the volume flow rate, the pump with circular-elliptic volute produces more head and has more efficiency than the rectangular one.

- Volute with rectangular cross sections has more surface, causing more skin friction and consequently less head and efficiency.

Further research works are planned to investigate the effect of multi geometrical parameters simultaneously, and analyze the interaction between these parameters.

## **References**

- [1] S. R. Shah, S. V. Jain, R. N. Patel, and V. J. Lakhera, "CFD for centrifugal pumps: a review of the state-of-the-art," 3rd Nirma University International Conference of Chemical, Civil and Mechanical Engineering, *Procedia Engineering*, vol. 51, 2013, pp. 715-720.
- [2] H. L. Stewart, *Pumps*, 3rd ed., Howard W. Sams & Co., 1981, Chap. 3.
- [3] E. Dick, J. Viereneels, S. Serbruyns, and J. Voorde, "Performance Prediction of Centrifugal Pumps with CFD-Tools," *Task Quarterly*, vol. 5, 2001, pp. 579-594.
- [4] K. Kaupert, P. Holbein, T. Staubli, "A First Analysis of Flow Field Hysteresis in a Pump Impeller," *Journal of Fluids Engineering*, vol. 118, 1996, pp. 685-692.
- [5] I. Potts, T. Newton, "Use of commercial CFD pack-age to predict shut-off behavior of model centrifugal pump: an appraisal," *I. Mech. E Seminar*, 1998.
- [6] J. Sun, H. Tsukamoto, "Off-Design Performance Prediction for Diffuser Pumps," *Journal of Power and Energy, Proceedings of I. Mech. E*, vol. 215, 2001, pp. 191-201.
- [7] F. A. Varley, "Effects of impeller design and surface roughness on the performance of centrifugal pumps," *Proceedings of the Institution of Mechanical Engineers*, vol. 175, 1961, pp. 955-989.
- [8] H. B. Jin, M. J. Kim, W. J. Chung, "A Study on the Effect of Variation of the Cross-sectional Area of Spiral Volute Casing for Centrifugal Pump," *World Academy of Science, Engineering and Technology*, vol. 68, 2012, pp. 2218-2227.
- [9] W. G. Li, "The Sudden-Rising head effect in centrifugal oil pumps," *World Pumps*, 2000, pp. 34-36.
- [10] Fluent Inc., <http://www.fluent.com/>.
- [11] J. Sun, and H. Tsukamoto, "Off-design performance prediction for diffuser pumps," *Journal of Power and Energy, Proceedings of I. Mech. E.*, vol. 215, 2001, pp. 191-201.
- [12] J. Gonzalez, J. Fernandez, E. Blanco, and C. Santolaria, "Numerical simulation of the dynamic effects due to impeller-volute interaction in a centrifugal pump," *ASME Journal of Fluids Engineering*, vol. 124, 2002, pp. 348-355.